島根大学地球資源環境学研究報告　34, 31～39 ページ（2016 年 3 月）
Geoscience Rept. Shimane Univ., 34, p.31～39（2016）

Article

Amphiboles from the kyanite–garnet amphibolite in the Tonaru metagabbro mass, Sambagawa metamorphic belt, central Shikoku, Japan

Md. Fazle Kabir*, Akira Takasu*, Hiroaki Matsuura* and Itsuki Kuraya*

Abstract

The Tonaru metagabbro mass occurs as a large lenticular body in the highest-grade (oligoclase-biotite zone) portions of the Sambagawa schists in the Besshi district. The Tonaru mass consists of diopside amphibolite and garnet-epidote amphibolite accompanied by small amounts of eclogite and marble. Kyanite–garnet amphibolites from the Tonaru metagabbro mass are composed of amphibole (calcic-amphibole; magnesiohornblende, actinolite, tremolite and tschermakite), zoisite, kyanite, garnet, phengite, paragonite, margarite, chlorite, quartz and pyrite. Amphiboles in the kyanite–garnet amphibolite exhibit three different modes of occurrence (Amp1-3). Amphiboles (Amp1) occur as inclusions in the porphyroblastic garnets are calcic in compositions (magnesiohornblende, actinolite and tremolite). Some are zoned, with magnesiohornblende core and actinolite/tremolite rim. Amphiboles (Amp2) in the matrix are mostly magnesiohornblende, and are zoned with magnesiohornblende core and actinolite/tschermakite rim. Amphiboles (Amp3) filling the fractures of the garnets are magnesiohornblende and tschermakite, and display a compositional zoning with magnesiohornblende core and tschermakite rim. The metamorphic evolution of the kyanite–garnet amphibolite from the Tonaru metagabbro mass is probably divided into two metamorphic events. The amphiboles (Amp1, 2) represent prograde metamorphism from the epidote–blueschist facies to the peak eclogite facies metamorphism. The actinolite rim of both occurrences suggests a retrograde metamorphism after the peak conditions. Amphiboles (Amp3) occur in fractures of the porphyroblastic garnets, and provide evidence of the second high-*P* metamorphic event. This metamorphic event is similar to that of the prograde Sambagawa metamorphism of the oligoclase-biotite zone.

Key words: Sambagawa (Sanbagawa) metamorphic belt, Tonaru metagabbro mass, amphibole, high-Mg garnet, kyanite

Introduction

The Sambagawa metamorphic belt extends for about 800 km throughout southwest Japan, stretching from Saganoseki Peninsula in Kyushu to the Kanto Mountains in the northeast (Fig. 1). Most parts of the Sambagawa belt underwent high-*P/T* metamorphism during the Cretaceous period (Itaya and Takasugi, 1988; Takasu and Dallmeyer, 1990; Wallis *et al.*, 2009). In the Besshi district of the Sambagawa belt the metamorphism is divided into four zones based on index minerals in the pelitic schists, namely the chlorite, garnet, albite-biotite, and oligoclase-biotite zones (Fig. 1; Enami, 1983; Higashino, 1990; Enami *et al.*, 1994). The higher-grade albite-biotite and oligoclase-biotite zones are equivalent to epidote–amphibolite facies metamorphism. Several eclogite-bearing bodies occur in the higher-grade albite-biotite and the oligoclase-biotite zones in the Besshi district, such as the Higashi-akaishi and Nikubuchi peridotite bodies, the Western Iratsu, Quartz Eclogite, Seba eclogitic basic schists, and the Sebadani, Eastern Iratsu and Tonaru metagabbro masses (e.g. Yokoyama, 1980; Takasu, 1984; Kunugiza *et al.*, 1986; Aoya, 2001; Kugimiya and Takasu, 2002; Ota *et al.*, 2004; Miyagi and Takasu, 2005, 1989; Kabir and Takasu, 2010; Endo and Tsuboi, 2013) (Fig. 1).

The Tonaru metagabbro mass (~6.5 km × 1 km) is one of the eclogite-bearing bodies located in the central part of the Besshi district, and lies within the oligoclase-biotite zone of the Sambagawa sequence (Higashino, 1990) (Fig. 1). Compositional banding that reflects the original igneous layered structure is widely developed in the mass, with schistosity defined by epidote–amphibolite facies minerals. The Tonaru metagabbro mass is considered to be derived from a layered gabbro (Banno *et al.*, 1976; Kunugiza *et al.*, 1986; Takasu, 1989). The Tonaru mass occurs as a large lenticular body consisting of diopside amphibolite (T-I type amphibolite) with small amounts of associated serpentinite, and garnet–epidote amphibolite (T-II type amphibolite) accompanied by small amounts of eclogite (Moriyama, 1990) (Fig. 2). Kunugiza (1984) suggested that serpentinites within the diopside amphibolites were originally peridotites that were serpentinized, followed by subsequent prograde metamorphism. Takasu *et al.* (1994) suggested that the eclogite-bearing garnet–epidote amphibolites underwent eclogite facies metamorphism before being retrograded into the epidote–amphibolite facies.

Miyagi and Takasu (2005) reported detailed petrology and a metamorphic history of the Tonaru metagabbro mass. They suggested that the Tonaru metagabbro mass underwent three metamorphic events. Precursor metamorphic event (i) of high-*T* amphibolite facies that occurred before the eclogite facies metamorphism is characterized by pargasite–taramite inclusions in the porphyroblastic garnets and Mg-rich relict cores of garnet (MgO ~ 8 wt%). The first

* Department of Geoscience, Graduate School of Science and Engineering, Shimane University, 1060 Nishikawatsu, Matsue 690-8504, Japan

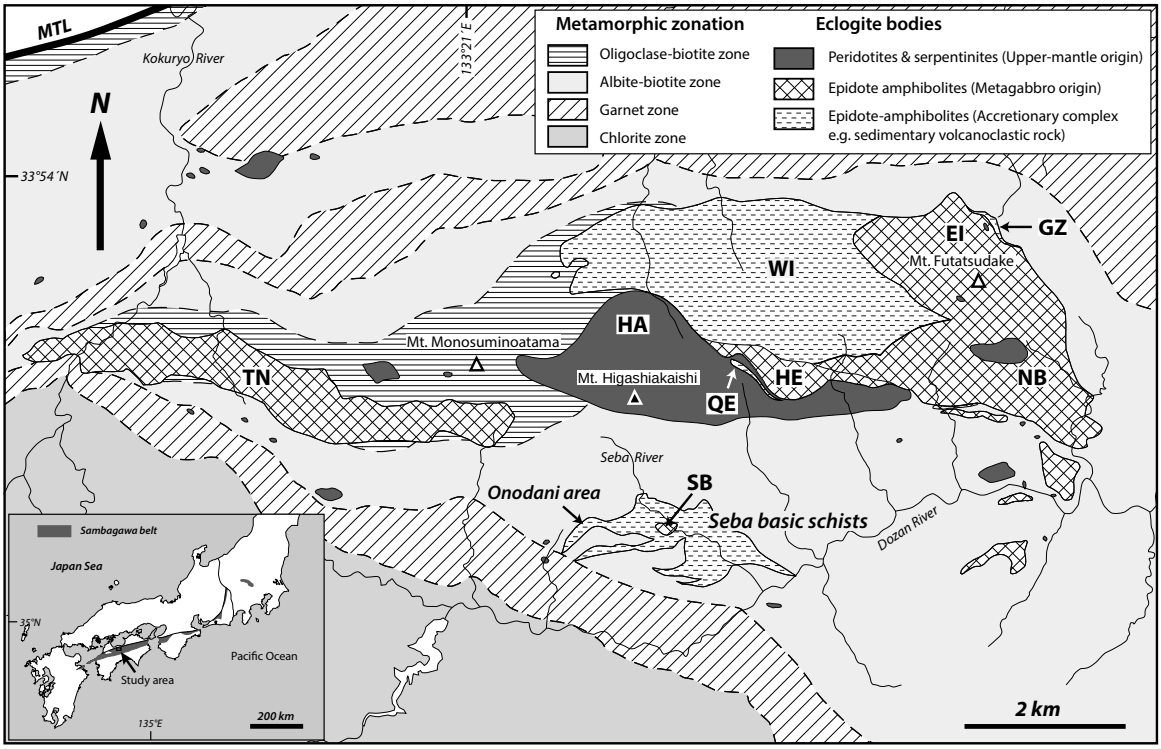

Fig. 1. Geological and metamorphic zonation map of the Sambagawa metamorphic belt in the Besshi district, central Shikoku, Japan (compiled from Takasu and Makino, 1980; Takasu, 1989; Higashino, 1990; Kugimiya and Takasu, 2002; Sakurai and Takasu, 2009; Kabir and Takasu, 2010). SB, Sebadani metagabbro mass; SEB, Seba basic eclogitic schists; TN, Tonaru metagabbro mass; WI, Western Iratsu mass; EI, Eastern Iratsu mass; HA, Higashi-akaishi peridotite mass; HE, Hornblende eclogite mass; NB, Nikubuchi peridotite mass; MTL, Median Tectonic Line.

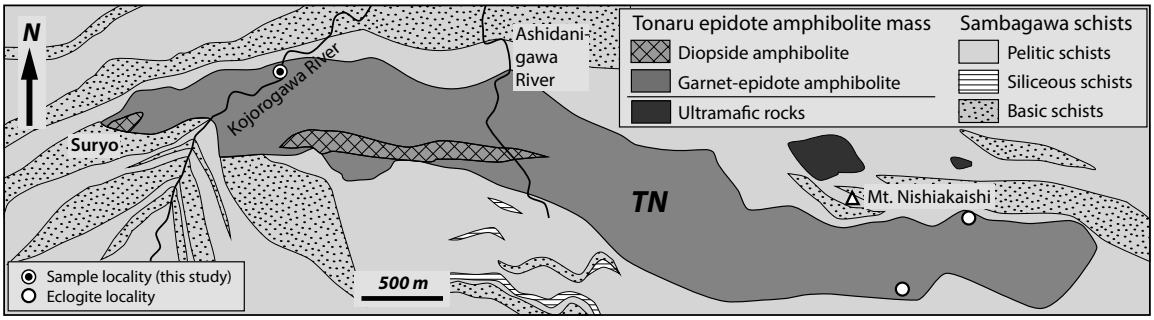

Fig. 2. Lithological map of the Tonaru metagabbro mass (after Miyagi and Takasu, 2005), with sample location. Eclogite localities of Kohsaka and Toriumi (1984) and Miyagi and Takasu (2005) are also shown.

high-*P* metamorphic event of the eclogite facies (ii) led to prograde metamorphism from the epidote–blueschist facies (300-450˚C and 7-11 kbar) to the eclogite facies (700-730˚C and ≥ 15 kbar), and subsequent retrogression into epidote–amphibolite facies. The mass subsequently underwent another prograde metamorphism (iii) together with the surrounding Sambagawa schists, reaching oligoclase–biotite zone metamorphic conditions.

In this study we describe the texture, modes of occurrence and the chemical compositions of amphiboles in high-Mg garnet- and kyanite-bearing garnet amphibolite (hereafter kyanite–garnet amphibolite) from the western part of the Tonaru metagabbro mass. Detail petrography of the kyanite–garnet amphibolite has been described by Matsuura *et al.* (2013). Amphiboles in the kyanite–garnet amphibolite display three different modes of occurrence (Amp1-3). Amphiboles (Amp1) occur as inclusions in the porphyroblastic garnets are subhedral prismatic crystals up to 0.7 mm long. They are calcic amphiboles (magnesiohornblende, actinolite and tremolite) (Figs. 3a and b). Some are zoned, with magnesiohornblende core and actinolite/tremolite rim (Fig. 3b). Amphiboles (Amp2) are mostly magnesiohornblende and occur as subhedral to anhedral prismatic grains up to 4 mm long in the matrix (Figs. 3c and d). Some of them are zoned, with magnesiohornblende core and actinolite/tschermakite rim (Fig. 3d). They contain inclusions of kyanite, Fe-garnet,

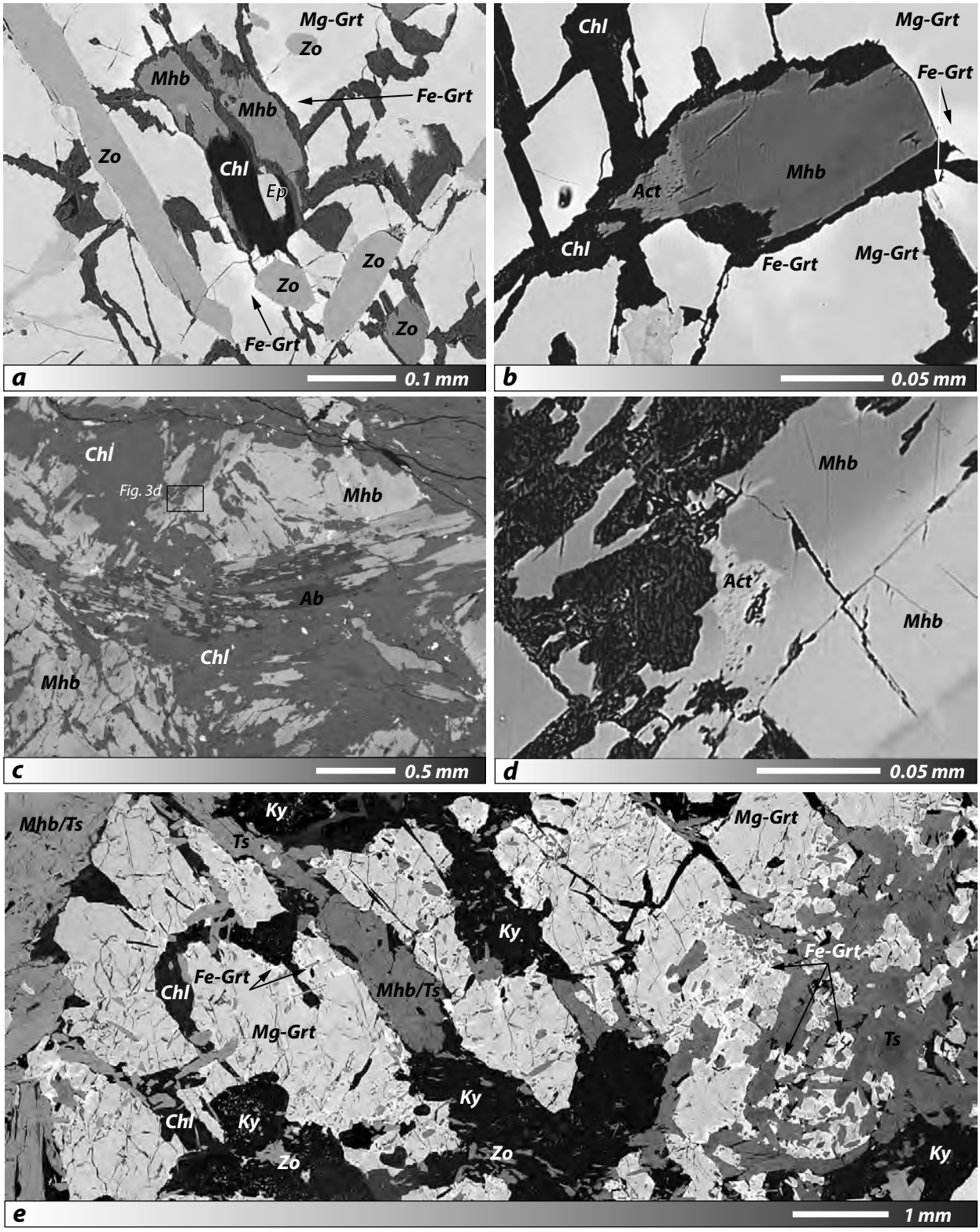

Fig. 3. Backscattered electron (BSE) images of the kyanite–garnet amphibolite from the Tonaru metagabbro mass. (a) High-Mg garnet (relatively lighter vein is Fe-rich garnet) contains inclusions of amphibole (Amp1, magnesiohornblende), zoisite, epidote and chlorite. (b) High-Mg garnet contains inclusions of amphibole (Amp1: magnesiohornblende core to actinolite rim) and chlorites fill the cracks of the garnet. (c) Schistosity-forming amphiboles (Amp2) are replaced by chlorite and albite. (d) Matrix amphibole (Amp2) is rimmed by actinolite. (e) The garnet contains fine-grained inclusions of zoisite. Fractures in the garnets are filled by kyanite, chlorite, zoisite and amphibole (Amp3: magnesiohornblende, tschermakite).

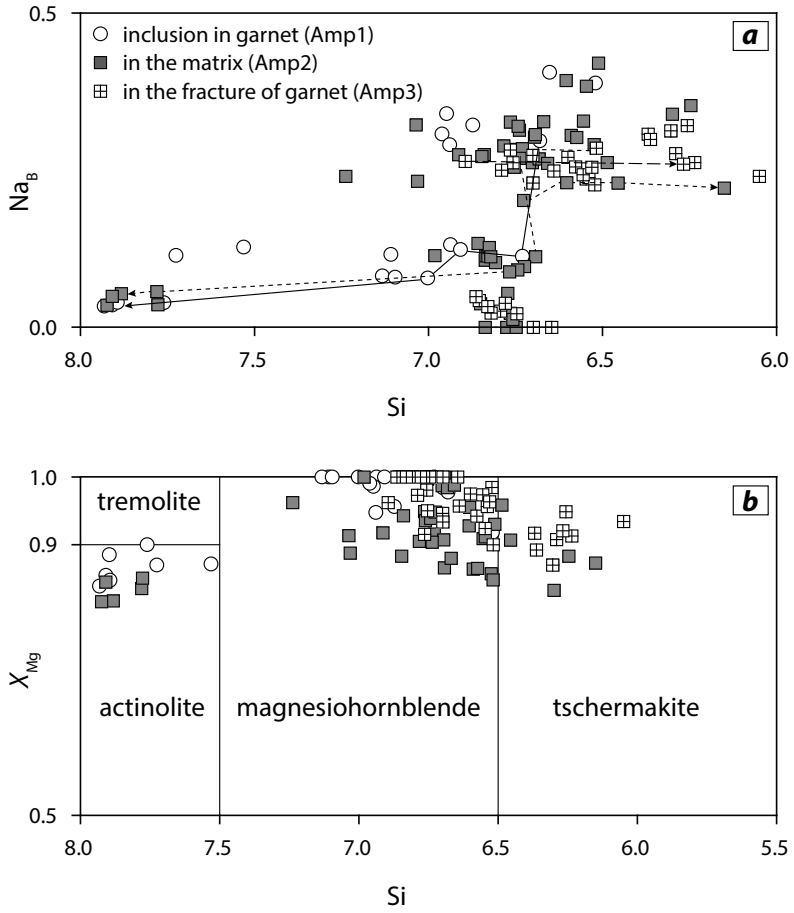

Fig. 4. Chemical compositions of amphiboles from the kyanite–garnet amphibolites. Arrows indicate core to rim zoning of Amp1, Amp2 and Amp3.

zoisite, phengite (Si 6.85-6.90 pfu) chlorite and quartz. Amphiboles (Amp3) filling the fractures of the garnets (magnesiohornblende, tschermakite) are anhedral in shape, and also display the similar compositional zoning as the matrix amphiboles (Amp2) (Fig. 3e). The mineral abbreviations used in the text, table, and figures follow Whitney and Evans (2010).

Chemical compositions of amphiboles

Chemical compositions of the amphiboles in the kyanite–garnet amphibolite from the western parts of the Tonaru metagabbro mass were investigated in Shimane University, using JEOL JXA 8800M and JXA 8530F electron microprobe analyzers. Analytical conditions used for quantitative analysis were 15 kV accelerating voltage, 20 nA specimen current, and 5 μm beam diameter. Correction procedure was carried out as described by Bence and Albee (1968). Fe^{3+} of amphibole is estimated using the 13eCNK method (Leake *et al.*, 1997).

Amphibole (Amp1) inclusions in the porphyroblastic garnet are classified as magnesiohornblende, actinolite and tremolite, with ranges of Si 6.52-7.93 per formula unit (pfu), Na_B 0.03-0.41 pfu, X_{Mg} (Mg / Mg + Fe^{2+}) 0.84-1, Ti 0-0.02 pfu and Al^{IV} 0.06-1.01 pfu. Amp1 is sometimes zoned, from magnesiohornblende core to actinolite / tremolite rims, increasing in Si (6.70-7.93 pfu), and decreasing Na_B (0.26-0.03 pfu), X_{Mg} (1-0.84), Ti (0.01-0 pfu) and Al^{VI} (0.81-0.06 pfu) (Fig. 4; Table 1).

Amphiboles (Amp2) in the matrix are classified as calcic amphiboles (magnesiohornblende, actinolite and tschermakite), with a wide ranges of Si 6.15-7.92 pfu, Na_B 0-0.42 pfu, X_{Mg} 0.82-1, Ti 0-0.02 pfu and Al^{VI} 0.05-1.15 pfu. The cores of the zoned amphiboles (Amp2) are classified as magnesiohornblende with Si 6.52-7.03 pfu, Na_B 0.09-0.31 pfu, X_{Mg} 0.85-1 and Al^{VI} 0.61-1 pfu, rimed by actinolite, with higher Si 7.78-7.92 pfu and lower Na_B 0.04-0.06 pfu, X_{Mg} 0.82-0.84 and Al^{VI} 0.08-0.11 pfu (Fig. 4). Some other zoned amphiboles (Amp2) are zoned from magnesiohornblende core to tschermakite rim, decreasing in Si (6.73-6.15 pfu) and X_{Mg} (0.95-0.87) and increasing Na_B (0.20-0.22 pfu) and Al^{VI} (0.60-0.99 pfu).

Amphiboles (Amp3) occurring in the garnet fractures are classified as magnesiohornblende, tschermakite with Si 6.05-6.91 pfu, Na_B 0-0.36 pfu, X_{Mg} 0.87-1, Ti 0-0.02 pfu and Al^{VI} 0.52-1.05 pfu. Some of these are zoned, magnesiohornblende core with Si 6.75-6.90 pfu, Na_B 0.26-0.27 pfu, X_{Mg} 0.95-0.96

and Al^{VI} 0.51-0.67 pfu and tschermakite rim with lower Si 6.24-6.37 pfu and X_{Mg} 0.91-0.92 and higher Na_B 0.26-0.31 pfu and Al^{VI} 0.96-1.05 pfu (Fig. 4).

Discussion and Conclusions

Amphiboles in the kyanite–garnet amphibolite from the Tonaru metagabbro mass exhibit several modes of occurrence and a wide range of chemical compositions, and they provide important information of diverse *P-T* conditions on the Sambagawa metamorphism.

The core of the amphiboles (Amp1) as inclusions in the porphyroblastic garnets and the core of the amphibole (Amp2) in the matrix are similar in compositions (magnesiohornblende), and probably share the same metamorphism. The actinolite rims of both amphiboles (Amp1 and 2) suggest similar retrograde metamorphic process. Amphibole (Amp3) occurring in the fractures of the garnets is also magnesiohornblende, which is rimmed by tschermakite. The tschermakite rims of the amphiboles (Amp2 and 3) are probably formed during another metamorphic event.

Based on petrography and chemical compositions of the constituent minerals, the metamorphic evolution of the kyanite–garnet amphibolites from the Tonaru metagabbro mass is divided into two events. These are a first high-pressure metamorphic event (i) represented by inclusions of amphiboles (Amp1) in the garnets and matrix amphiboles (Amp2), and a second high-pressure metamorphic event (ii) recorded by amphiboles (Amp3) developed in the fractures of the garnets and the rim of the matrix amphibole (Amp2). Matsuura *et al.* (2013) reported high-Mg garnets from the kyanite–bearing garnet amphibolites show a prograde zoning and the rim of the garnet records the evidence of the peak metamorphic stage of eclogite facies. Miyagi and Takasu (2005) reported a *P-T* path of eclogites. The prograde *P-T* trajectory passing through epidote–blueschist facies to eclogite facies of the peak conditions at 700-730˚C and ≥ 15 kbar, is followed by retrograde metamorphism into epidote–amphibolite facies. The amphiboles (Amp1 and 2) probably follow a similar prograde, peak and retrograde *P-T* path of the Tonaru eclogites and garnet–amphibolites described by Miyagi and Takasu (2005). Amphiboles (Amp3) developed as fracture-filling minerals provide evidence of the second high-*P* metamorphic event, and the rim of the matrix amphiboles (Amp2) also follow similar metamorphism. This metamorphic event is similar to that of the prograde metamorphism of the Sambagawa schists in the oligoclase-biotite zone, as already reported by Miyagi and Takasu (2005).

Acknowledgements

We thank the members of the Metamorphic Geology Seminar of Shimane University for discussion and helpful suggestion. We also thank Prof. Masahide Akasaka for constructive comments and Prof. Hiroaki Komuro for editorial reading on the manuscript. This study was partly supported by JSPS KAKENHI Grant (No. 24340123) to A.T.

References

Aoya, M., 2001, *P-T-D* path of eclogite from the Sambagawa belt deduced from combination of petrological and microstructural analyses. *Journal of Petrology*, **42**, 1225-1248.

Banno, S., Yokohama, K., Enami, M., Iwata, O., Nakamura, K. and Kasashima, S., 1976, Petrography of the peridotite-metagabbro complex in the vicinity of Mt. Higashi-akaishi, Central Shikoku. Part I. Megascopic textures of the Iratsu and Tonaru epidote amphibolite masses. *The Science Reports of Kanazawa University*, **21**, 139-159.

Enami, M., 1983, Petrology of pelitic schists in the oligoclase-biotite zone of the Sanbagawa metamorphic terrain, Japan: phase equilibria in the highest grade zone of a high-pressure intermediate type of metamorphic belt. *Journal of Metamorphic Geology*, **1**, 141-161.

Enami, M., Wallis, S. R. and Banno, Y., 1994, Paragenesis of sodic pyroxene-bearing quartz schists: implications for the *P-T* history of the Sanbagawa belt. *Contributions to Mineralogy and Petrology*, **116**, 182-198.

Endo, S. and Tsuboi, M., 2013, Petrogenesis and implications of jadeite-bearing kyanite eclogite from the Sanbagawa belt (SW Japan). *Journal of Metamorphic Geology*, **31**, 647-661.

Higashino, T., 1990, The higher grade metamorphic zonation of the Sambagawa metamorphic belt in central Shikoku, Japan. *Journal of Metamorphic Geology*, **8**, 413-423.

Itaya, T. and Takasugi, H., 1988, Muscovite K-Ar ages of the Sanbagawa schists, Japan and argon depletion during cooling and deformation. *Contributions to Mineralogy and Petrology*, **100**, 281-290.

Kabir, M. F. and Takasu, A., 2010, Evidence for multiple burial–partial exhumation cycles from the Onodani eclogites in the Sambagawa metamorphic belt, central Shikoku, Japan. *Journal of Metamorphic Geology*, **28**, 873-893.

Kohsaka, Y. and Toriumi, M., 1984, Deformation and recrystallization of the Tonaru amphibolite mass. *92nd Annual Meeting of the Geological Society of Japan*, 380.

Kugimiya, Y. and Takasu, A., 2002, Geology of the Western Iratsu mass within the tectonic melange zone in the Sambagawa metamorphic belt, Besshi district, central Shikoku, Japan. *Journal of the Geological Society of Japan*, **108**, 644-662.

Kunugiza, K., 1984, Metamorphism and origin of ultramafic bodies of the Sanbagawa Metamorphic Belt in central Shikoku. *Journal of the Japanese Association for Mineralogists, Petrologists and Economic Geologists*, **79**, 20-32.

Kunugiza, K., Takasu, A. and Banno, S., 1986, The origin and metamorphic history of the ultramafic and metagabbro bodies in the Sanbagawa Metamorphic Belt. *Geological Society of America Memoir*, **164**, 375-386.

Leake, B. E., Woolley, A. R., Arps, C. E. R., Birch, W. D., Gilbert, M. C., Grice, J. D., Hawthorne, F. C., Kato, A., Kisch, H. J., Krivovichev, V. G., Linthout, K., Laird, J., Mandarino, J. A., Maresch, W. V., Nickel, E. H., Rock, N. M. S., Schumacher, J. C., Smith, D. C., Stephenson, N. C. N., Ungaretti, L., Whittaker, E. J. W. and Youzhi, G., 1997, Nomenclature of amphiboles: report of the subcommittee on amphiboles of the International Mineralogical Association, Commission on New Minerals and Mineral Names. *The Canadian Mineralogist*, **35**, 219-246.

Matsuura, H., Takasu, A. and Kabir, M. F., 2013, High–Mg garnets in kyanite garnet amphibolite from the Tonaru metagabbro mass in the Sambagawa metamorphic belt, Besshi district, central Shikoku, Japan. *Geoscience Reports of Shimane University, Japan*, **32**, 13-22.

Miyagi, Y. and Takasu, A., 2005, Prograde eclogites from the Tonaru epidote amphibolite mass in the Sambagawa Metamorphic Belt, central Shikoku, southwest Japan. *Island Arc*, **14**, 215-235.

Moriyama, H., 1990, Two metamorphic paths in the Tonaru epidote amphibolite mass within the Sambagawa belt, Besshi district, central Shikoku. *Geoscience Reports of Shimane University, Japan*, **9**, 49-54.

Ota, T., Terabayashi, M. and Katayama, I., 2004, Thermobaric structure and

metamorphic evolution of the Iratsu eclogite body in the Sanbagawa belt, central Shikoku, Japan. *Lithos*, **73**, 95-126.

Sakurai, T. and Takasu, A., 2009, Geology and metamorphism of the Gazo mass (eclogite-bearing tectonic block) in the Sambagawa metamorphic belt, Besshi district, central Shikoku, Japan. *Journal of Geological Society of Japan*, **115**, 101-121.

Takasu, A., 1984, Prograde and retrograde eclogites in the Sambagawa metamorphic belt, Besshi district, Japan. *Journal of Petrology*, **25**, 619-643.

Takasu, A., 1989, *P-T* histories of peridotite and amphibolite tectonic blocks in the Sanbagawa metamorphic belt, Japan. In: *Evolution of Metamorphic Belts* (eds Daly, J. S., Cliff, R. A. & Yardley, B. W. D.), Geological Society, London, Special Publications, **43**, 533-538, Blackwell Scientific Publications, Oxford.

Takasu, A. and Dallmeyer, R. D., 1990, $^{40}Ar/^{39}Ar$ mineral age constraints for the tectonothermal evolution of the Sambagawa metamorphic belt, central Shikoku, Japan: a Cretaceous accretionary prism. *Tectonophysics*, **185**, 111-139.

Takasu, A. and Makino, K., 1980, Stratigraphy and geologic structure of the Sanbagawa metamorphic belt in the Besshi district, Shikoku, Japan (Reexamination of the recumbent fold structures). *Earth Science*, **34**, 16-26 (in Japanese with English abstract).

Takasu, A., Wallis, S. R., Banno, S. and Dallmeyer, R. D., 1994, Evolution of the Sambagawa metamorphic belt, Japan. *Lithos*, **33**, 119-133.

Wallis, S. R., Anczkiewicz, R., Endo, S., Aoya, M., Platt, J. P., Thirlwall, M. and Hirata, T., 2009, Plate movements, ductile deformation and geochronology of the Sanbagawa belt, SW Japan: tectonic significance of 89-88 Ma Lu–Hf eclogite ages. *Journal of Metamorphic Geology*, **27**, 93-105.

Whitney, D. L. and Evans, B. W., 2010, Abbreviations for names of rock-forming minerals. *American Mineralogist*, **95**, 185-187.

Yokoyama, K., 1980, Nikubuchi peridotite body in the Sanbagawa metamorphic belt; thermal history of the 'Al-pyroxene-rich suite'peridotite body in high pressure metamorphic terrain. *Contributions to Mineralogy and Petrology*, **73**, 1-13.

(Received: Nov. 27, 2015, Accepted: Dec. 9, 2015)

（要　旨）

Kabir, Md. Fazle・高須　晃・松浦弘明・蔵谷　樹，2016．四国中央部三波川変成帯東平変斑れい岩中の藍晶石ざくろ石角閃岩中の角閃石．島根大学地球資源環境学研究報告，34，31-39.

東平変斑れい岩体は別子地域の三波川帯の最高変成度地域（オリゴクレース－黒雲母帯）に巨大なレンズ型の岩体として分布する．この岩体は主要には透輝石角閃岩とざくろ石緑れん石角閃岩からなるが，少量のエクロジャイトと大理石を伴う．東平岩体には藍晶石を伴うざくろ石緑れん石角閃岩（藍晶石ざくろ石角閃岩）が産出し，この岩相は角閃石（Ca 角閃石：マグネシオホルンブレンド，アクチノ閃石，トレモラ閃石，チェルマック閃石），ゾイサイト，藍晶石，ざくろ石，フェンジャイト，パラゴナイト，マーガライト，緑泥石，石英，黄鉄鉱からなる．藍晶石ざくろ石角閃岩中の角閃石は 3 種の産状を示す（Amp1-3）．Amp1 は斑状変晶ざくろ石中の包有物で，組成は Ca 角閃岩（マグネシオリーベック閃石，アクチノ閃石，トレモラ閃石）である．Amp1 はマグネシオホルンブレンドの核部からアクチノ閃石またはチェルマック閃石の縁部への累帯構造を示すことがある．Amp2 は基質部に産し，組成は大部分がマグネシオホルンブレンドであり，マグネシオホルンブレンドの核部からアクチノ閃石またはトレモラ閃石の縁部への累帯構造を示すことがある．Amp3 はざくろ石の割れ目を充たす角閃岩で，マグネシオホルンブレンドとチェルマック閃石の組成を示す．マグネシオホルンブレンドの核部からチェルマック閃石の縁部への累帯構造を示すことがある．藍晶石ざくろ石角閃岩の変成履歴は 2 回の変成イベントに区分できる．Amp1 と Amp2 は緑れん石青色片岩相からピーク変成作用への昇温期変成作用の際に形成された．これらの角閃岩のアクチノ閃石の縁部はピーク変成条件後の降温期変成作用で形成されたと考えられる．Amp3 は 2 回目の高圧型変成作用によって形成された．この変成イベントはオリゴクレース黒雲母帯の三波川変成岩が受けた昇温期変成作用に類似する．

Table 1. Representative chemical compositions of amphiboles from the kyanite–garnet amphibolites.

Sample	140531-3																			
Analysis	4	5	6	7	8	16	26	51	52	53	54	56	59	62	63	81	82	99	102
Mode	In Grt	In Grt	In Grt	In Grt	In Grt	In Grt	In Grt	In Grt	In Grt	In Grt	In Grt	In Grt	In Grt	In Grt	In Grt	In Grt	In Grt	Matrix	Matrix
	Amp1	Amp1	Amp1	Amp1	Amp1	Amp1	Amp1	Amp1	Amp1	Amp1	Amp1	Amp1	Amp1	Amp1	Amp1	Amp1	Amp1	Amp2	Amp2
	Mhb	Act	Mhb	Tr	Mhb	Mhb	Mhb	Mhb	Mhb	Mhb	Act	Act	Mhb	Mhb	Act	Mhb	Act	Mhb	Mhb
	Core	Rim	Core	Rim				Core	→	→	Rim	Rim		Core	Rim	Core	Rim		Core
SiO_2	49.90	57.21	48.61	55.19	51.21	49.49	48.38	48.23	49.40	50.11	56.72	54.56	51.22	50.93	54.28	50.66	56.60	48.59	47.59
TiO_2	0.13	0.00	0.10	0.00	0.05	0.09	0.00	0.04	0.05	0.04	0.01	0.00	0.11	0.15	0.04	0.12	0.00	0.14	0.09
Al_2O_3	11.73	0.83	12.97	1.78	10.17	10.93	13.24	13.88	12.15	10.93	1.04	3.19	9.55	9.84	4.92	10.61	1.11	11.98	13.92
Cr_2O_3	0.00	0.00	0.02	0.00	0.00	0.00	0.00	0.00	0.01	0.00	0.00	0.01	0.01	0.03	0.00	0.00	0.01	0.00	0.00
MnO	0.07	0.16	0.01	0.22	0.08	0.10	0.08	0.10	0.12	0.10	0.24	0.21	0.07	0.10	0.18	0.11	0.22	0.11	0.04
MgO	17.64	19.40	17.25	19.13	17.76	16.59	16.66	16.67	17.13	17.76	19.28	18.38	18.54	18.34	18.64	17.48	19.48	16.09	17.15
CaO	11.03	12.90	11.75	12.21	11.20	11.28	11.51	11.09	11.12	11.42	12.61	11.99	11.63	11.62	12.59	11.29	12.94	11.22	11.44
Na_2O	1.49	0.13	1.51	0.14	1.21	1.28	1.59	1.71	1.50	1.24	0.13	0.42	1.07	1.10	0.60	1.29	0.15	1.44	1.82
K_2O	0.22	0.01	0.12	0.01	0.10	0.11	0.03	0.08	0.06	0.04	0.02	0.03	0.11	0.10	0.03	0.08	0.02	0.10	0.11
Total	98.12	98.42	97.87	96.40	98.30	97.47	97.78	98.07	97.58	97.57	97.62	95.84	97.57	97.64	98.03	98.06	97.78	97.43	96.89
O	23	23	23	23	23	23	23	23	23	23	23	23	23	23	23	23	23	23	24
Si	6.94	7.93	6.70	7.76	7.11	6.87	6.68	6.73	6.91	7.00	7.91	7.73	7.13	7.10	7.53	6.95	7.89	6.76	6.69
Ti	0.01	0.00	0.01	0.00	0.01	0.01	0.00	0.00	0.01	0.00	0.00	0.00	0.01	0.02	0.00	0.01	0.00	0.01	0.01
Al^{IV}	1.06	0.07	1.30	0.24	0.89	1.13	1.32	1.27	1.09	1.00	0.09	0.27	0.87	0.90	0.47	1.05	0.11	1.24	1.31
Al^{VI}	0.86	0.07	0.81	0.06	0.77	0.66	0.84	1.01	0.91	0.80	0.08	0.26	0.70	0.71	0.34	0.66	0.08	0.73	1.00
Cr	0.00	0.00	0.00	0.00	0.00	0.00	0.00	0.00	0.00	0.00	0.00	0.00	0.00	0.00	0.00	0.00	0.00	0.00	0.00
Fe^{2+}	0.00	0.77	0.06	0.45	0.00	0.16	0.08	0.00	0.00	0.00	0.68	0.58	0.00	0.00	0.57	0.05	0.73	0.18	0.00
Mn	0.01	0.02	0.00	0.03	0.01	0.01	0.01	0.01	0.01	0.01	0.03	0.03	0.01	0.01	0.02	0.01	0.03	0.01	0.01
Mg	3.66	4.01	3.54	4.01	3.68	3.43	3.43	3.47	3.57	3.70	4.01	3.88	3.85	3.81	3.86	3.57	4.05	3.34	3.60
Ca	1.64	1.92	1.74	1.84	1.67	1.68	1.70	1.66	1.67	1.71	1.88	1.82	1.74	1.74	1.87	1.66	1.93	1.67	1.72
Na^{B}	0.13	0.03	0.26	0.04	0.12	0.32	0.30	0.11	0.12	0.08	0.04	0.11	0.08	0.08	0.13	0.34	0.04	0.33	0.11
Na^{A}	0.27	0.00	0.14	0.00	0.21	0.02	0.13	0.35	0.28	0.26	0.00	0.00	0.21	0.22	0.03	0.00	0.00	0.06	0.38
K	0.04	0.00	0.02	0.00	0.02	0.02	0.01	0.01	0.01	0.01	0.00	0.00	0.02	0.02	0.01	0.01	0.00	0.02	0.02
Total	15.40	14.95	15.16	14.88	15.23	15.04	15.13	15.42	15.31	15.31	14.92	14.94	15.25	15.25	15.04	15.02	14.98	15.08	15.42
X_{Mg}	1.00	0.84	0.98	0.90	1.00	0.96	0.98	1.00	1.00	1.00	0.85	0.87	1.00	1.00	0.87	0.99	0.85	0.95	1.00

**Total Fe as FeO*
In Grt, inclusions in garnet

Sample	140531-3																			
Analysis	103	104	105	106	107	108	109	110	111	112	113	114	115	116	117	118	148	149	150
Mode	Matrix	Matrix	Matrix	Matrix	Matrix	Matrix	Matrix	Matrix	Matrix	Matrix	Matrix	Matrix	Matrix	Matrix	Matrix	Matrix	Matrix	Matrix	Matrix
	Amp2	Amp2	Amp2	Amp2	Amp2	Amp2	Amp2	Amp2	Amp2	Amp2	Amp2	Amp2	Amp2	Amp2	Amp2	Amp2	Amp2	Amp2	Amp2
	Mhb	Mhb	Mhb	Mhb	Mhb	Mhb	Mhb	Mhb	Mhb	Mhb	Mhb	Act	Act	Act	Mhb	Mhb	Mhb	Mhb	Mhb
	→	→	→	→	→	→	→	→	→	→	→	→	→	Rim			Core	→	→
SiO_2	47.96	48.29	48.14	48.50	48.48	48.13	50.21	46.89	46.49	46.15	45.98	55.11	55.35	54.69	47.79	47.62	48.71	48.65	48.59
TiO_2	0.13	0.12	0.12	0.05	0.12	0.09	0.05	0.08	0.08	0.09	0.09	0.01	0.00	0.02	0.11	0.10	0.11	0.09	0.14
Al_2O_3	13.53	13.25	13.04	13.03	12.77	12.53	9.58	14.17	14.11	14.67	14.66	1.37	1.07	1.81	13.11	13.19	12.37	12.37	12.41
Cr_2O_3	0.00	0.01	0.00	0.00	0.00	0.00	0.01	0.02	0.00	0.01	0.03	0.01	0.00	0.00	0.01	0.00	0.00	0.00	0.00
FeO*	4.87	5.04	4.81	4.92	6.16	7.74	8.14	8.75	8.96	8.88	9.15	7.88	7.73	8.10	4.95	4.86	4.75	4.44	4.66
MnO	0.03	0.03	0.05	0.03	0.08	0.10	0.10	0.16	0.17	0.17	0.15	0.22	0.17	0.27	0.00	0.05	0.01	0.01	0.02
MgO	17.38	17.52	17.47	17.48	16.36	15.73	16.37	14.36	14.17	14.00	13.81	18.36	18.51	18.47	17.12	17.20	17.76	17.89	17.80
CaO	11.47	11.58	11.55	11.74	11.49	11.45	11.78	11.25	11.20	11.28	11.29	12.64	12.70	12.72	11.56	11.61	11.44	11.45	11.33
Na_2O	1.70	1.73	1.60	1.67	1.54	1.47	1.01	1.82	1.75	1.80	1.77	0.19	0.13	0.21	1.65	1.70	1.64	1.72	1.68
K_2O	0.11	0.11	0.13	0.11	0.11	0.12	0.09	0.10	0.09	0.09	0.09	0.03	0.02	0.02	0.12	0.14	0.12	0.13	0.13
Total	97.17	97.69	96.90	97.53	97.09	97.37	97.33	97.58	97.00	97.14	97.00	95.81	95.68	96.30	96.40	96.47	96.92	96.74	96.77
O	23	23	23	23	23	23	23	23	23	23	23	23	23	23	23	23	23	23	23
Si	6.72	6.74	6.77	6.70	6.76	6.73	7.03	6.59	6.57	6.52	6.52	7.88	7.92	7.78	6.68	6.66	6.84	6.84	6.83
Ti	0.01	0.01	0.01	0.01	0.01	0.01	0.01	0.01	0.01	0.01	0.01	0.00	0.00	0.00	0.01	0.01	0.01	0.01	0.01
Al^{IV}	1.28	1.26	1.23	1.30	1.24	1.27	0.97	1.41	1.43	1.48	1.48	0.12	0.08	0.22	1.32	1.34	1.16	1.16	1.17
Cr	0.00	0.00	0.00	0.00	0.00	0.00	0.00	0.00	0.00	0.00	0.00	0.00	0.00	0.00	0.00	0.00	0.00	0.00	0.00
Al^{VI}	0.96	0.92	0.93	0.82	0.86	0.79	0.61	0.94	0.93	0.97	0.97	0.11	0.10	0.08	0.84	0.83	0.88	0.88	0.89
Fe^{3+}	0.63	0.61	0.60	0.52	0.48	0.60	0.52	0.56	0.59	0.56	0.56	0.07	0.03	0.19	0.52	0.53	0.60	0.57	0.63
Fe^{2+}	0.00	0.00	0.00	0.05	0.23	0.30	0.43	0.47	0.47	0.49	0.52	0.88	0.89	0.77	0.06	0.04	0.00	0.00	0.00
Mn	0.00	0.00	0.01	0.00	0.01	0.01	0.01	0.02	0.02	0.02	0.02	0.03	0.02	0.03	0.00	0.01	0.00	0.00	0.00
Mg	3.63	3.65	3.66	3.60	3.40	3.28	3.42	3.01	2.99	2.95	2.92	3.91	3.95	3.92	3.57	3.58	3.72	3.75	3.73
Ca	1.72	1.73	1.74	1.74	1.72	1.72	1.77	1.69	1.70	1.71	1.71	1.94	1.95	1.94	1.73	1.74	1.72	1.72	1.71
Na^{B}	0.10	0.09	0.09	0.26	0.28	0.28	0.23	0.31	0.30	0.29	0.29	0.05	0.04	0.06	0.27	0.26	0.11	0.11	0.11
Na^{A}	0.37	0.38	0.35	0.18	0.13	0.12	0.04	0.19	0.18	0.20	0.20	0.00	0.00	0.00	0.18	0.20	0.34	0.35	0.35
K	0.02	0.02	0.02	0.02	0.02	0.02	0.02	0.02	0.02	0.02	0.02	0.01	0.00	0.00	0.02	0.02	0.02	0.02	0.02
Total	15.45	15.42	15.40	15.20	15.15	15.14	15.06	15.21	15.19	15.22	15.22	15.00	14.99	15.00	15.20	15.23	15.40	15.42	15.45
X_{Mg}	1.00	1.00	1.00	0.99	0.94	0.92	0.89	0.86	0.87	0.86	0.85	0.82	0.82	0.84	0.98	0.99	1.00	1.00	1.00

**Total Fe as FeO*

Table 1. (continued)

Sample	140531-3																		
Analysis	151	152	153	154	155	156	157	158	159	160	162	163	165	166	168	170	45	46	47
Mode	Matrix	Matrix	Matrix	Matrix	Matrix	Matrix	Matrix	Matrix	Matrix	Matrix	Matrix	Matrix	Matrix	Matrix	Matrix	Matrix	Matrix	Matrix	Matrix
	Amp2	Amp2	Amp2	Amp2	Amp2	Amp2	Amp2	Amp2	Amp2	Amp2	Amp2	Amp2	Amp2	Amp2	Amp2	Amp2	Amp2	Amp2	Amp2
	Mhb	Mhb	Mhb	Mhb	Mhb	Mhb	Act	Mhb	Mhb	Mhb	Mhb	Mhb	Mhb	Mhb	Mhb	Mhb	Mhb	Act	Mhb
	→	→	→	→	→	→	Rim										Core	Rim	
SiO_2	48.81	48.61	48.50	51.87	46.34	48.14	55.50	46.86	47.77	47.89	47.08	47.14	47.99	49.57	48.08	48.63	49.06	55.55	47.99
TiO_2	0.12	0.14	0.15	0.05	0.10	0.12	0.04	0.09	0.10	0.10	0.13	0.08	0.11	0.11	0.09	0.11	0.11	0.03	0.13
Al_2O_3	12.35	12.48	10.88	7.18	14.10	11.54	1.19	12.53	12.18	12.15	12.95	13.28	12.15	11.13	12.61	12.54	11.87	1.67	11.85
Cr_2O_3	0.00	0.00	0.00	0.00	0.00	0.00	0.00	0.00	0.01	0.00	0.03	0.01	0.02	0.02	0.00	0.01	0.05	0.00	0.00
FeO*	4.54	4.79	7.27	6.86	8.55	7.73	7.11	8.03	7.46	7.50	8.51	8.47	7.59	4.64	5.03	5.02	5.33	8.64	8.49
MnO	0.02	0.02	0.15	0.18	0.14	0.10	0.16	0.14	0.09	0.07	0.15	0.15	0.11	0.05	0.08	0.02	0.05	0.19	0.16
MgO	17.67	17.64	16.46	18.04	14.50	15.45	18.93	15.06	15.85	15.54	14.58	14.65	15.89	18.04	17.30	17.57	18.34	18.74	15.64
CaO	11.39	11.36	11.41	11.45	11.03	11.34	12.48	11.09	11.16	11.28	11.12	11.03	11.16	11.28	11.33	11.41	11.33	12.65	11.51
Na_2O	1.69	1.78	1.33	0.89	1.66	1.40	0.18	1.58	1.48	1.43	1.72	1.78	1.54	1.37	1.63	1.70	1.38	0.13	1.48
K_2O	0.13	0.13	0.11	0.08	0.08	0.10	0.01	0.09	0.13	0.13	0.10	0.10	0.13	0.11	0.12	0.13	0.11	0.04	0.14
Total	96.71	96.94	96.26	96.61	96.48	95.91	95.59	95.46	96.23	96.09	96.38	96.68	96.69	96.31	96.26	97.14	97.62	97.64	97.38
O	23	23	23	23	23	23	23	23	23	23	23	23	23	23	23	23	23	23	23
Si	6.86	6.83	6.84	7.24	6.55	6.85	7.91	6.70	6.74	6.78	6.69	6.67	6.74	6.98	6.81	6.82	6.85	7.78	6.74
Ti	0.01	0.01	0.02	0.01	0.01	0.01	0.00	0.01	0.01	0.01	0.01	0.01	0.01	0.01	0.01	0.01	0.01	0.00	0.01
Al^{IV}	1.14	1.17	1.16	0.76	1.45	1.15	0.09	1.30	1.26	1.22	1.31	1.33	1.26	1.02	1.19	1.18	1.15	0.22	1.26
Al^{VI}	0.90	0.89	0.65	0.42	0.90	0.78	0.11	0.81	0.76	0.81	0.86	0.88	0.75	0.83	0.91	0.89	0.80	0.05	0.70
Cr	0.00	0.00	0.00	0.00	0.00	0.00	0.00	0.00	0.00	0.00	0.00	0.00	0.00	0.00	0.00	0.00	0.00	0.00	0.00
Fe^{3+}	0.53	0.57	0.65	0.65	0.71	0.49	0.11	0.63	0.67	0.54	0.53	0.58	0.68	0.64	0.62	0.60	0.93	0.33	0.65
Fe^{2+}	0.00	0.00	0.21	0.15	0.31	0.43	0.74	0.33	0.21	0.34	0.48	0.42	0.22	0.00	0.00	0.00	0.00	0.69	0.35
Mn	0.00	0.00	0.02	0.02	0.02	0.01	0.02	0.02	0.01	0.01	0.02	0.02	0.01	0.01	0.01	0.00	0.01	0.02	0.02
Mg	3.70	3.69	3.46	3.75	3.06	3.28	4.02	3.21	3.33	3.28	3.09	3.09	3.33	3.79	3.65	3.67	3.82	3.91	3.27
Ca	1.72	1.71	1.72	1.71	1.67	1.73	1.91	1.70	1.69	1.71	1.69	1.67	1.68	1.70	1.72	1.71	1.69	1.90	1.73
Na^{B}	0.13	0.13	0.28	0.24	0.33	0.27	0.05	0.30	0.31	0.29	0.31	0.33	0.32	0.11	0.10	0.11	0.04	0.04	0.27
Na^{A}	0.33	0.36	0.09	0.00	0.13	0.11	0.00	0.13	0.09	0.10	0.17	0.16	0.10	0.26	0.34	0.35	0.34	0.00	0.13
K	0.02	0.02	0.02	0.01	0.02	0.02	0.00	0.02	0.02	0.02	0.02	0.02	0.02	0.02	0.02	0.02	0.02	0.01	0.02
Total	15.34	15.39	15.11	14.97	15.14	15.13	14.96	15.15	15.11	15.13	15.19	15.18	15.12	15.37	15.39	15.39	15.66	14.94	15.16
X_{Mg}	1.00	1.00	0.94	0.96	0.91	0.88	0.85	0.91	0.94	0.91	0.87	0.88	0.94	1.00	1.00	1.00	1.00	0.85	0.90

**Total Fe as FeO*

Sample	MT-09071804																		
Analysis	4	40	51	57	36	41	37	38	6	44	1	2	3	4	67	79	80	81	82
Mode	Matrix	Matrix	In Grt	In Grt	In Grt	In Grt	Matrix	Matrix	Matrix	Matrix	Matrix	Matrix	Grt Fr	Grt Fr	Matrix	Matrix	Matrix	Matrix	Matrix
	Amp2	Amp2	Amp1	Amp1	Amp1	Amp1	Amp2	Amp2	Amp2	Amp2	Amp2	Amp2	Amp3	Amp3	Amp2	Amp2	Amp2	Amp2	Amp2
	Mhb	Mhb	Mhb	Mhb	Mhb	Mhb	Mhb	Mhb	Mhb	Mhb	Mhb	Ts	Mhb	Ts	Ts	Mhb	Mhb	Mhb	Mhb
											Core	Rim	Core	Rim	Rim	←	Core	Core	→
SiO_2	50.50	46.29	48.63	50.75	49.56	46.51	46.43	47.23	44.72	44.12	49.37	46.42	47.47	44.66	43.49	48.37	47.99	47.40	46.83
TiO_2	0.10	0.02	0.01	0.09	0.12	0.00	0.04	0.00	0.00	0.05	0.08	0.14	0.14	0.05	0.06	0.14	0.10	0.12	0.10
Al_2O_3	9.62	14.68	13.50	10.65	10.63	14.92	14.11	13.84	17.15	16.81	10.04	13.99	11.47	16.13	17.08	11.24	11.54	11.90	12.19
Cr_2O_3	0.03	0.00	0.00	0.00	0.14	0.00	0.00	0.00	0.00	0.00	0.01	0.00	0.00	0.02	0.00	0.00	0.04	0.00	0.00
FeO*	8.15	9.07	7.88	5.52	6.36	8.73	9.15	8.92	10.22	9.92	8.53	7.60	7.92	9.94	9.79	5.05	6.39	5.59	8.01
MnO	0.15	0.10	0.15	0.05	0.10	0.11	0.21	0.17	0.17	0.15	0.19	0.20	0.14	0.21	0.18	0.08	0.17	0.08	0.17
MgO	16.39	14.19	15.95	17.95	16.87	14.24	14.28	14.64	12.52	13.04	16.28	15.77	16.29	13.34	13.37	18.27	17.75	17.79	16.16
CaO	11.24	10.48	10.88	11.51	11.39	10.72	10.70	10.72	11.00	10.86	11.50	11.61	11.71	11.15	11.74	12.02	12.02	11.90	11.71
Na_2O	1.19	1.90	1.58	1.26	1.22	1.78	1.85	1.74	1.94	2.07	1.24	1.65	1.49	1.96	1.86	1.41	1.46	1.46	1.46
K_2O	0.11	0.12	0.09	0.12	0.15	0.16	0.16	0.11	0.16	0.12	0.09	0.16	0.14	0.17	0.15	0.18	0.16	0.18	0.14
Total	97.46	96.83	98.66	97.89	96.53	97.17	96.92	97.37	97.89	97.14	97.33	97.52	96.76	97.63	97.71	96.76	97.63	96.42	96.76
O	23	23	23	23	23	23	23	23	23	23	23	23	23	23	23	23	23	23	23
Si	7.04	6.51	6.65	6.96	6.94	6.52	6.55	6.60	6.30	6.25	6.91	6.49	6.70	6.30	6.15	6.84	6.77	6.75	6.60
Ti	0.01	0.00	0.00	0.01	0.01	0.00	0.00	0.00	0.00	0.01	0.01	0.01	0.01	0.01	0.01	0.02	0.01	0.01	0.01
Al^{IV}	0.96	1.49	1.35	1.04	1.06	1.48	1.45	1.40	1.70	1.75	1.09	1.51	1.30	1.70	1.85	1.16	1.23	1.25	1.40
Al^{VI}	0.62	0.95	0.83	0.68	0.69	0.99	0.89	0.88	1.15	1.05	0.57	0.79	0.61	0.99	1.00	0.71	0.69	0.75	0.63
Cr	0.00	0.00	0.00	0.00	0.02	0.00	0.00	0.00	0.00	0.00	0.00	0.00	0.00	0.00	0.00	0.00	0.00	0.00	0.00
Fe^{3+}	0.63	0.84	0.90	0.60	0.55	0.76	0.79	0.81	0.68	0.81	0.69	0.75	0.69	0.75	0.75	0.63	0.76	0.72	0.79
Fe^{2+}	0.32	0.22	0.01	0.03	0.19	0.27	0.29	0.24	0.53	0.36	0.31	0.14	0.24	0.42	0.41	0.00	0.00	0.00	0.16
Mn	0.02	0.01	0.02	0.01	0.01	0.01	0.02	0.02	0.02	0.02	0.02	0.02	0.02	0.03	0.02	0.01	0.02	0.01	0.02
Mg	3.40	2.97	3.25	3.67	3.52	2.98	3.00	3.05	2.63	2.75	3.40	3.28	3.43	2.81	2.82	3.85	3.74	3.77	3.40
Ca	1.68	1.58	1.59	1.69	1.71	1.61	1.62	1.61	1.66	1.65	1.73	1.74	1.77	1.69	1.78	1.82	1.82	1.82	1.77
Na^{B}	0.32	0.42	0.41	0.31	0.29	0.39	0.38	0.39	0.34	0.35	0.27	0.26	0.23	0.31	0.22	0.00	0.00	0.00	0.23
Na^{A}	0.00	0.10	0.01	0.03	0.04	0.10	0.12	0.08	0.19	0.21	0.06	0.18	0.18	0.22	0.29	0.39	0.40	0.40	0.17
K	0.02	0.02	0.01	0.02	0.03	0.03	0.03	0.02	0.03	0.02	0.02	0.03	0.03	0.03	0.03	0.03	0.03	0.03	0.02
Total	15.02	15.12	15.03	15.05	15.07	15.12	15.15	15.10	15.22	15.24	15.08	15.21	15.20	15.26	15.31	15.46	15.48	15.52	15.19
X_{Mg}	0.91	0.93	1.00	0.99	0.95	0.92	0.91	0.93	0.83	0.88	0.92	0.96	0.93	0.87	0.87	1.00	1.00	1.00	0.96

**Total Fe as FeO*

Grt Fr, garnet fracture

Table 1. (continued)

Sample	MT-09071804																		
Analysis	83	84	97	98	99	100	101	102	103	104	105	107	108	109	110	111	112	113	72
Mode	Matrix	Matrix	Matrix	Matrix	Matrix	Matrix	Grt Fr	Grt Fr	Grt Fr	Grt Fr	Grt Fr	Grt Fr	Grt Fr	Grt Fr	Grt Fr	Grt Fr	Grt Fr	Grt Fr	Grt Fr
	Amp2	Amp2	Amp2	Amp2	Amp2	Amp2	Amp3	Amp3	Amp3	Amp3	Amp3	Amp3	Amp3	Amp3	Amp3	Amp3	Amp3	Amp3	Amp3
	Ts	Mhb	Mhb	Mhb	Mhb	Mhb	Mhb	Mhb	Mhb	Mhb	Mhb	Ts	Ts	Mhb	Ts	Mhb	Ts	Ts	Ts
	→	→	→	→	→	Rim	Rim	←	←	←	←	←	Core	Core	Rim	Core	→	Rim	
SiO_2	45.97	47.96	47.21	47.26	47.48	47.14	47.10	47.51	47.78	48.52	47.82	45.23	44.40	48.54	43.91	48.12	43.30	43.65	47.31
TiO_2	0.11	0.10	0.09	0.12	0.12	0.07	0.11	0.09	0.06	0.11	0.06	0.05	0.07	0.09	0.03	0.06	0.07	0.03	0.06
Al_2O_3	14.48	11.36	11.29	12.22	12.20	12.10	12.32	12.08	12.36	11.82	11.90	15.60	16.14	9.69	16.08	11.28	16.57	16.22	12.58
Cr_2O_3	0.07	0.03	0.00	0.03	0.07	0.00	0.04	0.01	0.00	0.00	0.02	0.05	0.02	0.00	0.05	0.02	0.04	0.03	0.00
FeO*	8.46	7.36	5.50	5.25	5.53	6.00	5.63	6.47	5.10	4.74	8.38	8.70	8.82	7.58	8.92	7.96	8.10	7.96	9.97
MnO	0.21	0.14	0.03	0.02	0.05	0.06	0.04	0.04	0.08	0.00	0.13	0.17	0.26	0.18	0.21	0.13	0.15	0.12	0.11
MgO	14.86	16.75	17.21	17.32	17.49	17.16	17.31	16.90	17.68	18.37	15.94	14.23	13.87	16.78	13.87	16.35	13.73	14.07	14.94
CaO	11.77	11.96	11.38	11.49	11.55	11.61	11.48	11.46	11.54	11.83	11.50	11.22	11.35	11.41	11.00	11.55	11.26	11.31	11.46
Na_2O	1.59	1.29	1.44	1.62	1.49	1.53	1.52	1.41	1.51	1.45	1.28	1.81	1.79	1.16	1.76	1.32	1.80	1.84	1.70
K_2O	0.09	0.14	0.18	0.12	0.13	0.15	0.13	0.11	0.13	0.17	0.15	0.12	0.13	0.10	0.14	0.12	0.14	0.13	0.11
Total	97.60	97.09	94.33	95.44	96.10	95.82	95.67	96.07	96.25	97.00	97.18	97.18	96.85	95.51	95.97	96.92	95.15	95.35	98.25
O	23	23	23	23	23	23	23	23	23	23	23	23	23	23	23	23	23	23	23
Si	6.46	6.73	6.75	6.77	6.76	6.76	6.75	6.79	6.78	6.82	6.70	6.37	6.29	6.90	6.26	6.75	6.24	6.27	6.62
Ti	0.01	0.01	0.01	0.01	0.01	0.01	0.01	0.01	0.01	0.01	0.01	0.01	0.01	0.01	0.00	0.01	0.01	0.00	0.01
Al^{IV}	1.54	1.27	1.25	1.23	1.24	1.24	1.25	1.21	1.22	1.18	1.30	1.63	1.71	1.10	1.74	1.25	1.76	1.73	1.38
Al^{VI}	0.85	0.60	0.66	0.84	0.81	0.80	0.83	0.83	0.85	0.78	0.66	0.96	0.99	0.52	0.96	0.62	1.05	1.01	0.70
Cr	0.01	0.00	0.00	0.00	0.01	0.00	0.00	0.00	0.00	0.00	0.00	0.01	0.00	0.00	0.01	0.00	0.00	0.00	0.00
Fe^{3+}	0.67	0.67	0.65	0.64	0.75	0.71	0.76	0.76	0.72	0.68	0.79	0.76	0.75	0.76	0.90	0.76	0.70	0.70	0.75
Fe^{2+}	0.32	0.19	0.01	0.00	0.00	0.00	0.00	0.00	0.00	0.00	0.19	0.27	0.30	0.14	0.16	0.18	0.28	0.26	0.42
Mn	0.02	0.02	0.00	0.00	0.01	0.01	0.00	0.00	0.01	0.00	0.02	0.02	0.03	0.02	0.03	0.02	0.02	0.01	0.01
Mg	3.11	3.50	3.67	3.70	3.72	3.67	3.70	3.60	3.74	3.85	3.33	2.99	2.93	3.55	2.95	3.42	2.95	3.01	3.12
Ca	1.77	1.80	1.75	1.76	1.76	1.78	1.76	1.76	1.75	1.78	1.73	1.69	1.72	1.74	1.68	1.74	1.74	1.74	1.72
Na^{B}	0.23	0.20	0.25	0.05	0.02	0.01	0.02	0.03	0.04	0.02	0.27	0.31	0.28	0.26	0.32	0.26	0.26	0.26	0.28
Na^{A}	0.20	0.15	0.15	0.40	0.39	0.41	0.40	0.37	0.38	0.37	0.07	0.19	0.21	0.06	0.17	0.10	0.24	0.25	0.18
K	0.02	0.03	0.03	0.02	0.02	0.03	0.02	0.02	0.02	0.03	0.03	0.02	0.02	0.02	0.03	0.02	0.03	0.02	0.02
Total	15.22	15.17	15.18	15.42	15.50	15.43	15.50	15.37	15.52	15.53	15.10	15.21	15.24	15.07	15.19	15.12	15.27	15.27	15.20
X_{Mg}	0.91	0.95	1.00	1.00	1.00	1.00	1.00	1.00	1.00	1.00	0.95	0.92	0.91	0.96	0.95	0.95	0.91	0.92	0.88

**Total Fe as FeO*

Sample	MT-09071804																		
Analysis	73	74	75	76	77	78	79	80	81	82	84	85	86	87	88	89	90	123	125
Mode	Grt Fr	Grt Fr	Grt Fr	Grt Fr	Grt Fr	Grt Fr	Grt Fr	Grt Fr	Grt Fr	Grt Fr	Grt Fr	Grt Fr	Grt Fr	Grt Fr	Grt Fr	Grt Fr	Grt Fr	Grt Fr	Grt Fr
	Amp3	Amp3	Amp3	Amp3	Amp3	Amp3	Amp3	Amp3	Amp3	Amp3	Amp3	Amp3	Amp3	Amp3	Amp3	Amp3	Amp3	Amp3	Amp3
	Ts	Ts	Ts	Ts	Ts	Ts	Ts	Ts	Ts	Ts	Ts	Ts	Ts	Ts	Ts	Ts	Ts	Ts	Ts
SiO_2	48.18	48.99	49.37	47.78	46.22	46.42	47.07	46.58	45.27	42.30	48.51	48.65	49.20	49.10	49.02	47.52	46.80	48.16	44.66
TiO_2	0.11	0.05	0.08	0.12	0.13	0.14	0.09	0.13	0.09	0.07	0.12	0.16	0.11	0.14	0.16	0.13	0.11	0.14	0.05
Al_2O_3	11.58	10.88	10.04	12.10	14.09	13.99	13.54	12.86	14.90	18.63	11.85	11.65	11.54	11.28	11.50	13.18	13.16	11.63	16.13
Cr_2O_3	0.01	0.03	0.01	0.01	0.00	0.00	0.00	0.00	0.00	0.00	0.00	0.00	0.00	0.02	0.00	0.00	0.00	0.01	0.02
FeO*	8.84	9.04	8.53	7.48	8.08	7.60	6.53	8.48	9.97	9.51	8.24	5.84	5.29	6.22	5.18	6.41	7.44	6.35	9.94
MnO	0.16	0.15	0.19	0.17	0.18	0.20	0.07	0.12	0.20	0.06	0.14	0.04	0.03	0.06	0.07	0.11	0.08	0.03	0.21
MgO	15.58	15.93	16.28	16.27	15.43	15.77	16.41	15.46	13.81	8.96	15.87	17.56	18.27	17.61	18.15	16.77	15.98	17.43	13.34
CaO	11.68	11.65	11.50	11.62	10.94	11.61	11.68	11.62	11.38	15.92	11.50	11.68	11.94	11.81	11.79	11.62	11.59	11.42	11.15
Na_2O	1.52	1.29	1.24	1.55	1.65	1.65	1.79	1.75	1.85	0.98	1.41	1.62	1.60	1.53	1.54	1.78	1.69	1.49	1.96
K_2O	0.10	0.09	0.09	0.14	0.14	0.16	0.14	0.15	0.13	0.10	0.15	0.16	0.15	0.14	0.13	0.14	0.14	0.13	0.17
Total	97.76	98.10	97.33	97.24	96.86	97.52	97.30	97.14	97.59	96.53	97.77	97.35	98.12	97.89	97.54	97.66	96.99	96.78	97.63
O	23	23	23	23	23	23	23	23	23	23	23	23	23	23	23	23	23	23	23
Si	6.76	6.82	6.91	6.69	6.47	6.49	6.57	6.58	6.40	6.42	6.76	6.76	6.85	6.79	6.86	6.60	6.58	6.83	6.30
Ti	0.01	0.01	0.01	0.01	0.01	0.01	0.01	0.01	0.01	0.01	0.01	0.02	0.01	0.01	0.02	0.01	0.01	0.01	0.01
Al^{IV}	1.24	1.18	1.09	1.31	1.53	1.51	1.43	1.42	1.60	1.58	1.24	1.24	1.15	1.21	1.14	1.40	1.42	1.17	1.70
Al^{VI}	0.67	0.61	0.57	0.69	0.80	0.79	0.80	0.72	0.88	1.75	0.71	0.66	0.75	0.63	0.76	0.76	0.76	0.77	0.99
Cr	0.00	0.00	0.00	0.00	0.00	0.00	0.00	0.00	0.00	0.00	0.00	0.00	0.00	0.00	0.00	0.00	0.00	0.00	0.00
Fe^{3+}	0.60	0.71	0.69	0.66	0.94	0.75	0.60	0.66	0.73	1.67	0.66	0.61	0.61	0.62	0.63	0.66	0.67	0.80	0.75
Fe^{2+}	0.43	0.35	0.31	0.22	0.00	0.14	0.16	0.34	0.45	2.87	0.30	0.07	0.00	0.10	0.00	0.09	0.20	0.00	0.42
Mn	0.02	0.02	0.02	0.02	0.02	0.02	0.01	0.01	0.02	0.01	0.02	0.00	0.00	0.01	0.01	0.01	0.01	0.00	0.03
Mg	3.26	3.31	3.40	3.40	3.22	3.28	3.42	3.25	2.91	2.03	3.30	3.64	3.79	3.63	3.79	3.47	3.35	3.69	2.81
Ca	1.76	1.74	1.73	1.74	1.64	1.74	1.75	1.76	1.72	2.59	1.72	1.74	1.78	1.75	1.77	1.73	1.74	1.74	1.69
Na^{B}	0.24	0.26	0.27	0.26	0.36	0.26	0.25	0.24	0.28	0.00	0.28	0.26	0.04	0.25	0.05	0.27	0.26	0.03	0.31
Na^{A}	0.17	0.09	0.06	0.16	0.09	0.18	0.23	0.24	0.23	0.29	0.10	0.17	0.39	0.16	0.37	0.21	0.20	0.38	0.22
K	0.02	0.02	0.02	0.03	0.03	0.03	0.02	0.03	0.02	0.02	0.03	0.03	0.03	0.03	0.02	0.02	0.03	0.02	0.03
Total	15.19	15.10	15.08	15.19	15.12	15.21	15.26	15.26	15.25	15.89	15.12	15.20	15.41	15.18	15.42	15.23	15.23	15.45	15.26
X_{Mg}	0.88	0.91	0.92	0.94	1.00	0.96	0.96	0.90	0.87	0.41	0.92	0.98	1.00	0.97	1.00	0.98	0.94	1.00	0.87

**Total Fe as FeO*